it obeys, to an approximation, the WLF rate–temperature equation. This dependence has often been observed for ionic conduction.

Registry No. (Dimethyl terephthalate)·(1,4-butanediol)·(poly(tetramethylene oxide)) (copolymer), 9078-71-1.

References and Notes

(1) E. J. Roche and E. L. Thomas, *Polymer*, **22**, 333 (1981).
(2) R. G. Vadimsky, *Meth. Exp. Phys.*, **16**, 185 (1980).
(3) G. K. Hoeschele and W. K. Witsiepe, *Angew. Makromol. Chem.*, **29/30**, 267 (1973).
(4) R. W. Seymour, J. R. Overton, and L. S. Corley, *Macromolecules*, **8**, 331 (1975).
(5) A. Lilaonitkul, J. C. West, and S. L. Cooper, *J. Macromol. Sci., Phys.*, **B12**, 563 (1976).
(6) L. Zhu and G. Wegner, *Makromol. Chem.*, **182**, 3625 (1981).
(7) J. W. C. van Bogart, D. A. Bluemke, and S. L. Cooper, *Polymer*, **22**, 1428 (1981).
(8) M. Gordon and J. S. Taylor, *J. Appl. Chem.*, **2**, 493 (1952).
(9) M. Matsuo, K. Geshi, A. Moriyama, and C. Sawatari, *Macromolecules*, **15**, 193 (1982).
(10) L. Zhu, G. Wegner, and U. Bandara, *Makromol. Chem.*, **182**, 3639 (1981).
(11) U. Bandara and M. Droscher, *Colloid Polym. Sci.*, **261**, 26 (1983).
(12) L. E. Alexander, "X-Ray Diffraction Methods in Polymer Science", Wiley, New York, 1969, p 77.
(13) J. D. Lake, *Acta Crystallogr.*, **23**, 191 (1967).
(14) O. Kratky, I. Pilz, and P. J. Schmitz, *J. Colloid Interface Sci.*, **21**, 24 (1966).
(15) M. A. Vallance, D. C. Faith, III, and S. L. Cooper, *Rev. Sci. Instrum.*, **51**, 1338 (1980).
(16) M. A. Vallance and S. L. Cooper, In "Computer Applications in Applied Polymer Science", T. Provder, Ed., American Chemical Society, Washington, DC, 1982, ACS Symp. Ser. No. 197, p 277.
(17) P. J. Flory, *J. Chem. Phys.*, **17**, 223 (1949).
(18) J. Runt and I. R. Harrison, *Meth. of Exp. Phy.* **16**, 287 (1980).
(19) M. Gilbert and F. J. Hybart, *Polymer*, **13**, 327 (1972).
(20) J. D. Hoffman and J. J. Weeks, *J. Res. Natl. Bur. Stand., Sect. A*, **66**, 13 (1962).
(21) M. Yokouchi, Y. Sakakibara, Y. Chatani, J. Tadokoro, T. Tanaka, and K. Yoda, *Macromolecules*, **9**, 266 (1976).
(22) U. Alter and R. Bonart, *Colloid Polym. Sci.*, **254**, 348 (1976).
(23) R. Hosemann and S. N. Bagchi, "Direct Analysis of Diffraction by Matter", North-Holland, Amsterdam, 1962, p 216.
(24) J. Wang and I. R. Harrison, *Meth. Exp. Phys.*, **16**, 128 (1980).
(25) W. Ruland, *Acta Crystallogr.*, **14**, 1180 (1961).
(26) W. Ruland, *Acta Crystallogr.*, **23**, 302 (1967).
(27) A. M. North, R. A. Pethrick, and A. D. Wilson, *Polymer*, **19**, 923 (1978).
(28) A. Lilaonitkul and S. L. Cooper, *Macromolecules*, **12**, 1146 (1979).
(29) S. Saito, H. Sasabe, T. Nakajima, and K. Yada, *J. Polym. Sci., Part A-2*, **6**, 1297 (1968).
(30) H. Sasabe and S. Saito, *Polym. J. (Tokyo)*, **3**, 631 (1972).
(31) L. D. Stepin, *Sov. Phys.-Tech. Phys. (Engl. Transl.)*, **10**, 768 (1965).
(32) H. Pauly and H. P. Schwan, *Biophys. J.*, **6**, 621 (1966).
(33) K. Asami, T. Hanai, and N. Koizumi, *Jpn., J. Appl. Phys.*, **19**, 359 (1980).
(34) J. D. Ferry, "Viscoelastic Properties of Polymers", 3rd ed., Wiley, New York, 1980, p 264.
(35) J. D. Hoffman, *Polymer*, **24**, 3 (1983).
(36) C. M. Guttman, E. A. DiMarzio, and J. D. Hoffman, *Polymer*, **22**, 1466 (1981).
(37) M. A. Vallance, Preliminary Report, University of Wisconsin—Madison, 1982.
(38) W. F. Brown, Jr., *J. Chem. Phys.*, **23**, 1514 (1955).
(39) W. E. A. Davies, *J. Phys. D*, **4**, 318 (1971).

Diffraction by Aperiodic Polymer Chains: The Structure of Liquid Crystalline Copolyesters

John Blackwell,* Genaro A. Gutierrez, and Robin A. Chivers

Department of Macromolecular Science, Case Western Reserve University, Cleveland, Ohio 44106.

Received May 19, 1983

ABSTRACT: The X-ray diffraction data for stiff-chain liquid crystalline aromatic copolyesters have been interpreted by calculation of the scattering characteristics of random copolymer chains. The meridional region of fiber diagrams of copolymers of *p*-hydroxybenzoic acid (HBA), 2,6-dihydroxynaphthalene (DHN), and terephthalic acid (TPA) and copolymers of HBA and 2-hydroxy-6-naphthoic acid (HNA) contains maxima that are aperiodic and shift in their positions depending on the monomer ratio. We have shown that excellent agreement is obtained between the positions of these observed maxima and those predicted for an aperiodic array of points where each point represents a monomer in a random chain, separated from adjacent points by the appropriate monomer lengths. Extension of these calculations to atomic models for the copolymer chains shows that only small changes occur in the positions of the predicted maxima, but there is now reasonably good agreement between the observed and calculated intensities.

Introduction

Copolyesters of *p*-hydroxybenzoic acid (HBA) and similar components form liquid crystalline melts, and this property can be utilized, e.g., to form high-strength fibers and novel molded plastics. A large number of thermotropic copolyesters have been reported in the patent literature, and their structures and properties have been reviewed by Jin et al.[1] We are using X-ray diffraction to study the structure of two groups of wholly aromatic copolyesters: copolymers of HBA and 2-hydroxy-6-naphthoic acid (HNA) and copolymers of HBA, 2,6-dihydroxynaphthalene (DHN), and terephthalic acid (TPA).

Schematic of the X-ray diffraction patterns of melt-spun fibers of three monomer ratios for each copolymer system are shown in Figures 1 and 2. These patterns indicate a high degree of axial orientation. The presence of sharp equatorial reflections suggests some order to the lateral packing, but the diffuse equatorial scattering, especially for the HBA/DHN/TPA system, points to extensive lateral disorder. The most striking features of the X-ray data are that the meridional maxima are aperiodic and also vary in position with changes in the monomer ratio. Analytical methods yield little information about the monomer sequence distribution in the copolymers, but the X-ray data argue against extensive blockiness. Rather it appears that we are dealing with largely or completely random sequences. These wholly aromatic copolymers will adopt stiff extended-chain conformations, and this stiffness will probably be independent of the monomer sequence.

We have derived the diffraction characteristics of rigid aperiodic polymer chains and have shown that the data are compatible with completely random sequences. In this

0024-9297/84/2217-1219$01.50/0

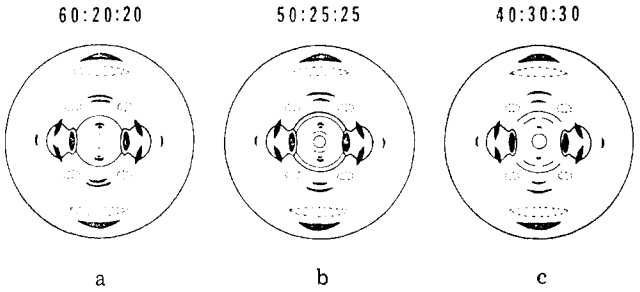

Figure 1. Schematics of X-ray fiber diffraction patterns of three HBA/DHN/TPA monomer ratios: (a) 60/20/20; (b) 50/25/25; (c) 40/30/30. The original patterns recorded on film are shown in ref 2.

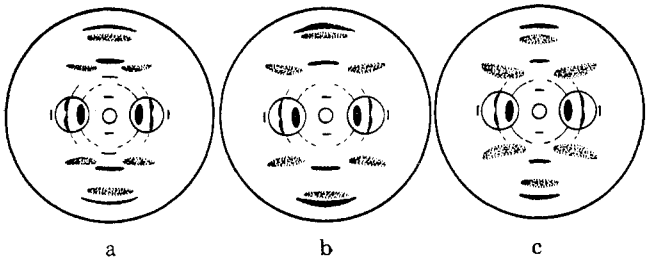

Figure 2. Schematics of X-ray fiber diffraction patterns of three HBA/HNA monomer ratios: (a) 30/70; (b) 58/42; (c) 75/25. The original patterns recorded on film are shown in ref 3.

paper we describe the methods used in these calculations and give examples of the results. We have taken the following approaches:

(i) A model for the polymer chain is set up by using a random number generator to determine the sequence and representing each monomer by a point.

(ii) The random number generator is replaced by calculation of the correlation function that describes the neighbor probabilities.

(iii) An atomic model is used instead of the point model for the chain in calculations i and ii.

Details of approach i for the two copolymer systems studied here have already been published.[2,3]

Experimental Section

Specimens of the copolyesters were supplied by Celanese Research Co., Summit, NJ, and had been synthesized as described by Calundann.[4,5] The HBA/DHN/TPA copolymer was supplied in three monomer ratios: 60/20/20, 50/25/25, and 40/30/30, each in the form of melt-spun fibers. Five monomer ratios for the HBA/HNA copolymer were supplied: 25/75, 30/70, 50/50, 58/42, and 75/25. Fibers were drawn from the molten chips with tweezers. X-ray data were recorded as described in ref 2 and 3.

Atomic models for the monomer residues were derived by using standard bond lengths and angles and were compatible with the structures determined by single-crystal methods for low molecular weight aromatic esters.[6,7] Planar aromatic and carboxyl groups were assumed, and the aromatic-carboxyl torsion angles were set at 30°, as suggested by model compounds and potential energy calculations.[8,9] Atomic models for the residues are shown in Figure 3; the lengths of the residues (ester oxygen to ester oxygen) were 6.35 Å for HBA, 7.15 Å for TPA, 7.85 Å for DHN, and 8.37 Å for HNA. The atomic coordinates for HBA and HNA used to calculate the transforms of the atomic model of copoly(HBA/HNA) are given in Table I. (Only the z coordinates are used in the present calculations.)

Experimental Results

Schematics of the X-ray fiber diagrams of the three HBA/DHN/TPA monomer ratios and the 30/70, 58/42, and 75/25 HBA/HNA copolymers are shown in Figures 1 and 2. The d spacings of the meridional maxima are given in Table II for HBA/HNA/TPA and in Table III

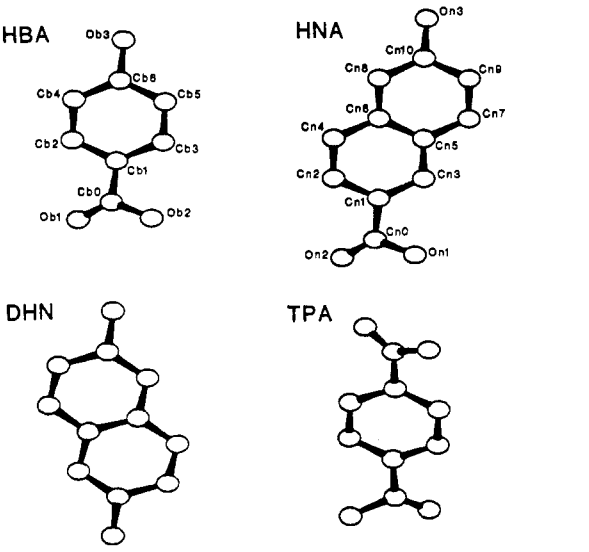

Figure 3. Projections of the monomer residue structures based on standard bond lengths and angles. The numbering of the atoms for HBA and HNA is the same as in Table I.

Table I
Atomic Coordinates

HBA	x	y	z
Ob1 ester oxygen	0.00	0.00	0.00
CbO carbonyl carbon	0.00	−1.14	0.77
Ob2 carbonyl oxygen	−0.02	−2.24	0.31
Cb1 phenyl carbon 1	0.03	−0.80	2.22
Cb2 phenyl carbon 2	0.63	0.36	2.72
Cb3 phenyl carbon 3	−0.59	−1.70	3.09
Cb4 phenyl carbon 4	0.62	0.62	4.09
Cb5 phenyl carbon 5	−0.61	−1.44	4.47
Cb6 phenyl carbon 6	0.00	−0.28	4.97
Ob3 ester oxygen	0.00	0.00	6.35
HNA	x	y	z
On1 ester oxygen	0.00	0.00	0.00
CnO carbonyl carbon	0.00	−1.25	0.56
On2 carbonyl oxygen	0.06	−2.25	−0.09
Cn1 naphthyl carbon 1	−0.09	−1.17	2.04
Cn2 naphthyl carbon 2	−0.72	−2.23	2.69
Cn3 naphthyl carbon 3	0.43	−0.10	2.77
Cn4 naphthyl carbon 4	−0.84	−2.23	4.09
Cn5 naphthyl carbon 5	0.32	−0.09	4.17
Cn6 naphthyl carbon 6	−0.32	−1.15	4.83
Cn7 naphthyl carbon 7	0.83	0.98	4.91
Cn8 naphthyl carbon 8	−0.44	−1.15	6.22
Cn9 naphthyl carbon 9	0.72	0.99	6.30
Cn10 naphthyl carbon 10	0.08	−0.07	6.96
On3 ester oxygen	0.00	0.00	8.37

for all five compositions of HBA/HNA.

Diffraction by Rigid Aperiodic Polymer Chains

Diffraction by rigid aperiodic polymer chains has not, to our knowledge, been considered previously. (There has, however, been a brief discussion of this problem for certain low molecular weight liquid crystalline structures.[10]) The meridional intensity distribution is derived from the projection of the entire structure onto the fiber axis, z. Figure 4a shows a typical short random sequence for the HBA/DHN/TPA copolymer. The meridional intensity, $I(Z)$, is given by $I(Z) \propto |F(Z)|^2$, where $F(Z)$ is the Z-axis Fourier transform of the structure. Z is the coordinate on the axis in reciprocal space corresponding to the chain axis; the constant of proportionality includes the Lorentz and polarization factors. $F_c(Z)$ for a particular chain is given by

$$F_c(Z) = \sum_j f_j \exp(2\pi i Z z_j) \qquad (1)$$

(a)

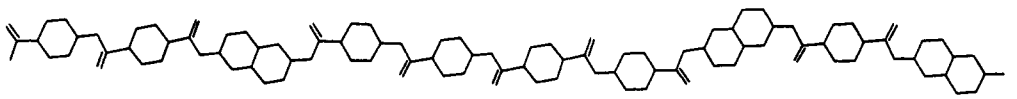

(b) • B • P • N • B • B • P • B • N • P • N •

Figure 4. (a) A short sequence of random monomer sequence for copoly(HBA/DHN/TPA) in a planar conformation. (b) Point model for the same copolymer sequence.

Table II

HBA/DHN/TPA	*d* spacings, Å: obsd[a]	calcd: point random	calcd: point conv
60/20/20	~6.8 (weak, diffuse)	6.76	6.76
	6.05 ± 0.05 (weak)		
	3.31 ± 0.03 (strong)	3.36	3.37
	2.98 ± 0.03 (strong)	3.09	3.08
	~2.3 (broad, diffuse)		
	2.01 ± 0.03 (very strong)	2.11	2.11
50/25/25	6.98 ± 0.07 (weak)	6.85	6.85
	~5.9 (weak, diffuse)		
	3.38 ± 0.03 (strong)	3.44	3.44
	2.97 ± 0.03 (strong)	3.05	3.05
	~2.3 (broad, diffuse)		
	2.02 ± 0.03 (very strong)	2.11	2.11
40/30/30	6.96 ± 0.05 (weak)	6.95	7.00
	3.48 ± 0.03 (strong)	3.50	3.51
	2.96 ± 0.03 (strong)	3.03	3.02
	~2.3 (broad, diffuse)	2.39	2.37
	2.00 ± 0.03 (strong)	2.11	2.11

[a] The relative intensities of the observed maxima are shown in parentheses.

Table III

HBA/HNA	exptl *d* spacings,[a] Å: film	exptl *d* spacings,[a] Å: diffractometer	calcd *d* spacings,[b] Å: atomic conv	calcd *d* spacings,[b] Å: point conv
25/75	8.09 ± 0.07	8.11 ± 0.07	8.09	7.98
	4.08 ± 0.04	4.15 ± 0.02	4.20	4.17
	2.77 ± 0.03	2.85 ± 0.01	2.85	2.84
	2.05 ± 0.03	2.09 ± 0.01	2.10	2.10
30/70	7.95	7.89	8.01	7.88
	4.11	4.09	4.21	4.17
	2.83	2.87	2.86	2.85
	2.06	2.09	2.10	2.10
50/50	7.43	7.49	7.61	7.41
			4.31	4.11
	2.84	2.95	2.95	2.93
	2.02	2.09	2.10	2.10
58/42	7.35	7.19	7.45	7.19
			4.40	4.01
	2.98	2.96	2.99	2.98
	2.05	2.08	2.11	2.10
75/25	6.78	6.70	7.04	6.75
	3.03	3.09	3.09	3.09
	2.03	2.09	2.11	2.11

[a] Experimental errors are given for the 25/75 preparation and are similar for the other compositions. [b] The positions of peak maxima have been interpolated from the discrete calculated points.

where f_j is the atomic scattering factor of the jth atom with z coordinate z_j and the summation is over all atoms in the chain. This needs to be averaged over all, or at least a large number, of the possible chain sequences and then compared with the meridional intensity distribution.

a. Point Model. These polymer chains are inevitably stiff and extended because of the 1,4-phenyl and 2,6-naphthyl linkages. Variation in the conformation can occur only by rotation about the aromatic–CO and O–aromatic bonds, which are approximately parallel to the chain axis (see Figure 4a). Hence the z-axis projections of the chains are approximately independent of their conformations. As a starting point for the calculations we have represented a chain by an aperiodic array of points, positioned for convenience at the ester oxygens, as shown in Figure 4b. The lengths of the different residues are taken as constant: the ester oxygen–ester oxygen vectors are assumed to be parallel to the chain axis. In the actual structure a distribution of residue lengths is to be expected, due to a range of torsional angles and axial inclination of the residues. The latter effect can be seen in Figure 4a and depends on the local monomer sequence. However, these are only minor effects because of the 1,4- and 2,6-linkage geometry.

This point approximation is trivial for a homopolymer, which can be regarded as the convolution of the monomer with a repeating (periodic) point lattice. The Fourier transform is given by

$$F_c(Z) = F_m(Z)F_l(Z) \tag{2}$$

where $F_m(Z)$ and $F_l(Z)$ are the Fourier transforms of the monomer and the lattice, respectively. $F_l(Z)$ is simply the Laue function, which samples the transform of the monomer at values of Z that correspond to $00l$ reflections for a crystalline homopolymer. Thus the positions of the maxima are determined by $F_l(Z)$, and their intensities depend on $F_m(Z)$. For the aperiodic chain the situation is more complicated because the successive monomers are not identical. However, for the present series of copolymers, the monomers are very similar to one another, and thus it is reasonable to expect that the Fourier transform for the aperiodic point lattice will contain peaks in approximately the same positions as those calculated for an atomic model of the chains, as is demonstrated by the results presented below.

The Fourier transform of linear array of N points with coordinates z_j is given by

$$F(Z) = \sum_{j=1}^{N} \exp(2\pi i Z z_j) \tag{3}$$

Our first procedure was to use a random number generator to set up the copolymer sequences. The computer programs take into account the monomer ratios, the allowed chemical combinations, and depletion of a limited number of reactant molecules. Reactivity ratios can also be varied in order to simulate blockiness (see below). In the initial calculations a completely random sequence was assumed. Figure 5 shows typical results for the HBA/DHN/TPA copolymers with the three available monomer compositions. The squared Fourier transforms are averaged over 200 chains of 10 monomers and are sampled at 0.001-Å^{-1} increments between 0 and 0.55 Å^{-1}. The computed transforms have been smoothed arithmetically to eliminate noise, which can also be reduced by averaging over more

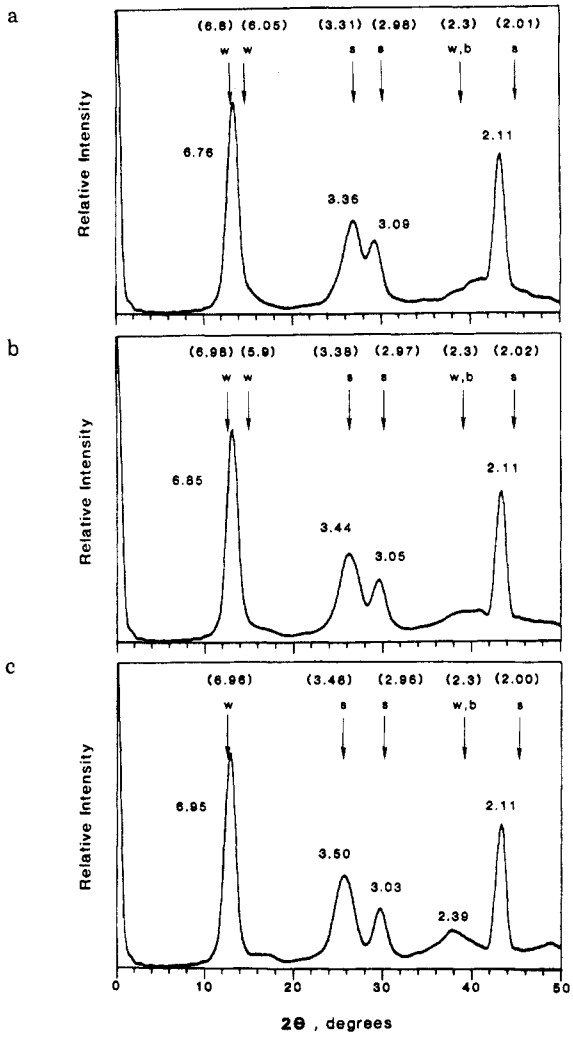

Figure 5. Squared averaged Fourier transforms of random point models for HBA/DHN/TPA copolymers at three monomer ratios: (a) 60/20/20; (b) 50/25/25; (c) 40/30/30. These data are averaged over 200 chains of 10 monomers and have been smoothed.

chains. Use of a longer chain results in a noisier transform, but the positions of the peaks are unaffected. The chain length (10 residues) corresponds more to a persistence length than to the degree of polymerization, which is approximately 150.

The positions of the observed and calculated maxima are compared in Figure 5 and Table II. It can be seen that the random point model has reproduced the basic features of the observed meridional intensity distribution, which contains three strong maxima: two in the 3.5–3.0-Å range and one at ~2 Å. We also observe one or two weak maxima in the 7–6-Å range and diffuse intensity centered at ~2.3 Å. The most striking change with monomer composition is that the two maxima in the 3-Å region move further apart as the HBA ratio decreases: the separation increases from 0.3 to 0.4 to 0.5 Å as the HBA content decreases from 60 to 50 to 40%. The calculated transforms contain peaks in the approximate positions of the observed reflections and reproduce the behavior of the doublet with considerable accuracy. It should be noted that the point approximation can only be expected to predict the *positions* of the maxima. The intensities will depend heavily on the intraresidue interferences and can only be compared in calculations for an atomic model for the chain.

The positions of the maxima in the transforms calculated based on models produced with the random number generator are subject to statistical variations to the extent that a limited sample is representative of a much larger

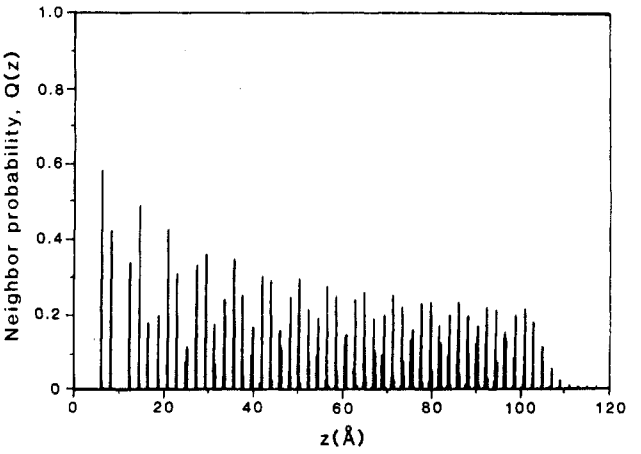

Figure 6. Neighbor probability distribution (autocorrelation) for a random chain of HBA/HNA 58/42 plotted out to the 14th neighbors of an infinite chain.

assembly. The calculated d spacings given in Table II are averages from six separate calculations, and the standard deviations are less than the experimental errors in the observed data. Small differences between these results and those published previously[2] also reflect the use of slightly different monomer lengths, based on improvements in the stereochemistry of the molecular models.

The above statistical variations are avoided by calculating the transforms from the correlation functions. Instead of deriving $I(Z)$ as $|F(Z)|^2$ with eq 3, one can compute the neighbor probability function $Q(z)$, which is the autocorrelation function of the chain. The intensity is then the Fourier transform of $Q(z)$:

$$I(Z) = \sum_j Q(z_j) \cos(2\pi Z z_j) \quad (4)$$

This procedure has the added advantage of requiring much less computer time. In the point model, $Q(z_j)$ is the probability of the existence of points separated by z_j anywhere along an infinite chain and is a centrosymmetric function. The computed $Q(z)$ for the HBA/HNA point model for the 58/42 monomer ratio is shown in Figure 6. Note that because of the way that the monomers are defined, with their origins at the ester oxygen, the first nearest neighbors, HBA–HNA and HNA–HNA, occur at the same z, as do HBA–HBA and HNA–HBA. The probabilities in Figure 6 are calculated out to the 14th neighbors in an infinite chain. In the transform calculations presented below we consider a limited chain length by multiplying $Q(z)$ by a triangular function.

Figure 7 shows the point autocorrelation transforms calculated for HBA/HNA copolymers at monomer ratios running from 100/0 [poly(HBA)] to 0/100 [poly(HNA)] in 10% increments. These transforms are for chains of 15 monomers. For poly(HBA) three maxima are predicted in the range out to d = 2 Å, which are orders of 6.35 Å, as is observed in electron diffraction patterns of the polymer.[11] Similarly, for poly(HNA) four maxima are seen within d = 2 Å that are orders of 8.37 Å. Across the composition range for the copolymers there is a steady transition from one extreme to the other. The maximum at $d \cong 2.1$ Å remains at approximately the same position throughout because the monomer lengths are fortuitously in the approximate ratio 3:4. The first two maxima for poly(HBA) move progressively to higher and lower d spacings with increasing HNA content, until, at 50/50, a fourth maximum develops at d = 4.17 Å.

This behavior is matched closely by the experimental results in Figure 2 and Table III. For the five monomer ratios the meridional d spacings move progressively with

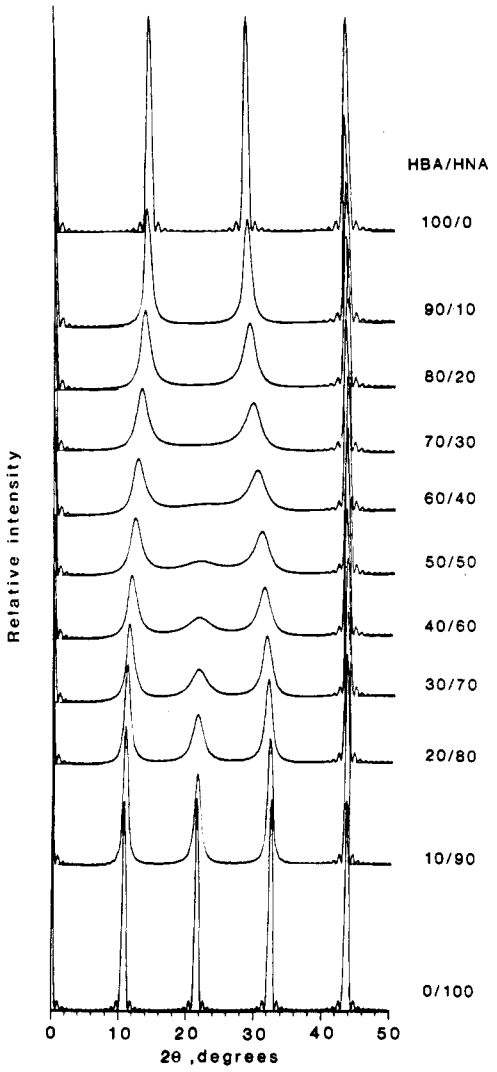

Figure 7. Fourier transforms of point autocorrelation functions for random HBA/HNA sequences for different monomer ratios between 0/100 and 100/0. The monomer ratios are indicated on the curves.

composition: four maxima are seen for both 25/75 and 30/70 and three for each of 50/50, 58/42, and 75/25. The agreement between the observed and calculated d spacings is very good, especially for the diffractometer data, where the smearing of the 2-Å layer line streak is minimized in the $\theta/2\theta$ scan. These data have previously been shown to be in agreement with the results from the random number approach.[3]

The excellent agreement shows that we can explain the diffraction characteristics of these copolymers by a model for a stiff chain of completely random monomer sequence. The random chain was generated by using a procedure that set the reactivity ratios at unity for all possible polymerization reactions. However, we have the ability to change the reactivity ratios and find that the calculated transforms are extremely sensitive to block copolymer character, such that all but minor deviations from a random sequence can be ruled out for the HBA/DHN/TPA copolymers. Details of the latter calculations will be published shortly.[12]

b. Atomic Model. The above calculations need to be extended to the atomic model for the chain, first to be sure that the same meridional maxima are predicted and second to attempt to reproduce the intensity distribution. Conversion of the random point model to the equivalent atomic model is achieved by adding the atoms for the appropriate residue to its origin ester oxygen. Equation 1, the summation over all atoms in the chain, is simplified by calculation of the Fourier transforms of the individual residues, $F_r(Z)$

$$F_r(Z) = \sum_{j=1}^{N_r} f_j \exp(2\pi i Z z_j) \tag{5}$$

where the summation is over all N atoms of the residue. The Fourier transform of the chain, $F_c(Z)$, is then given by

$$F_c(Z) = \sum_{k=1}^{N} F_{r,k}(Z) \exp(2\pi i Z z_k) \tag{6}$$

where $F_{r,k}(Z)$ is the Fourier transform of the kth residue (at coordinate z_k) and the summation is for a chain of N monomers. $|F_c(Z)|^2$ is then averaged over a number of chains before comparison with the observed data.

Alternatively, and preferably for the reasons given above, we can calculate the intensity from the autocorrelation function. The full expression for the Fourier transform of the autocorrelation function of the chain is

$$I(Z) = \sum_j \sum_k q_{jk} f_j f_k \exp(2\pi i Z z_{jk}) \tag{7}$$

where q_{jk} is the probability of atoms j and k at an axial separation of $z_{jk} = z_j - z_k$. This is simplified by using the autocorrelation function for the point model, $Q(z)$, which can be written

$$Q(z) = \sum_A \sum_B Q_{AB}(z) \tag{8}$$

where $Q_{AB}(z)$ is the probability of a residue of type B at a distance z from a residue of type A and the summations cover all possible pair relationships. $Q_{AB}(z)$ is nonzero at specific values of $z = z_l$. Conversion to the atomic model is achieved by multiplying the transform of $Q_{AB}(z)$ by $F_{AB}(Z)$, the transform of the convolution of residue B with residue A:

$$I(Z) = \sum_A \sum_B \sum_l Q_{AB}(z_l) F_{AB}(Z) \exp(2\pi i Z z_l) \tag{9}$$

where

$$F_{AB}(Z) = \sum_j \sum_k f_{A,j} f_{B,k} \exp[2\pi i Z (z_{B,k} - z_{A,j})] \tag{10}$$

The subscripts A,j and B,k designate the jth atom in residue A and the kth atom in residue B, respectively, when both residues have the same origin. Note that $F_{AB}(Z)$ is real for self-convolutions (A = B). Otherwise, $F_{AB}(Z)$ is complex, but the imaginary parts of eq 9 cancel out since $F_{AB}(Z) = F_{BA}^*(Z)$ (complex conjugate) and $Q_{AB}(z) = Q_{BA}(-z)$.

Figure 8 shows the computed transforms obtained by both methods for the atomic model of the 58/42 copolymer of HBA/HNA using the atomic coordinates listed in Table I. Both transforms are for chains of 10 residues; the transform for the random number model is averaged over 300 chains and has *not* been smoothed. The differences between the two transforms are very small and are due to the statistical deviations from randomness in the random number approach. The calculated intensities are corrected for the Lorentz and polarization effects to facilitate comparisons with the observed intensities. Figure 8 also shows an axial X-ray diffractometer $\theta/2\theta$ scan of the copolymer of the same composition. We have not yet made quantitative comparisons between these observed and calculated data, but qualitatively the intensity agreement can be seen to be very good. The positions of the observed and calculated peak maxima are compared in Table III, and in most cases are within 0.1 Å of each other. The subsidiary maxima occurring around the calculated curves are Fourier termination effects. These arise because the calculations

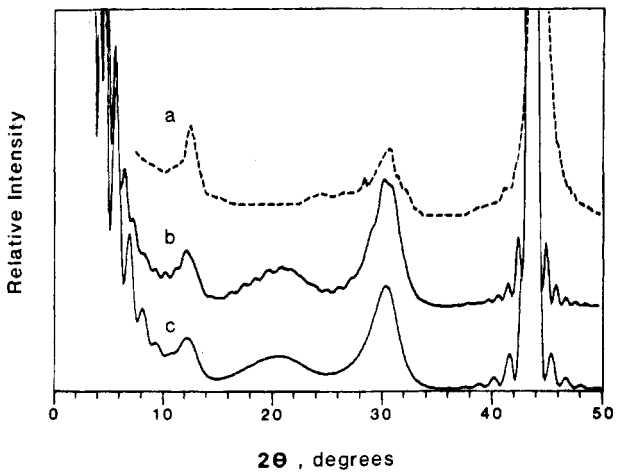

Figure 8. Comparison of experimental data and atomic model calculations for a random chain of 10 residues of HBA/HNA 58/42: (a) experimental diffractometer trace; (b) squared averaged Fourier transform of 300 chains produced by the random number generator (unsmoothed data); (c) the Fourier transform of the correlation function. The Lorentz/polarization correction has been applied to the calculated data, assuming the geometry of a $\theta/2\theta$ diffractometer scan.

are for monodisperse chains, and they can be greatly reduced by considering a distribution of chain lengths. This and other details of the work on both sets of copolymers will be described in future publications.

Conclusions

We have shown that the positions of the meridional maxima for the two stiff-chain copolyester systems vary with monomer ratio and that these can be predicted by calculations based on models for stiff chains of random monomer sequences. Simple models in which the monomers are approximated to points give excellent agreement between the observed and calculated d spacings. Statistical variations in the predicted peak positions that result from the use of a random number generator to set up the models of the chains are avoided by calculation of the intensity distribution via the autocorrelation function that describes the probability of monomer neighbors. Extension of the calculations to atomic models for the chains results in only minor changes in the peak positions but greatly improves the match between the observed and calculated intensities.

Although the differences between the observed and calculated d spacings are small, the agreement could be improved further by refinement of the monomer lengths. As noted above, the monomers are probably not exactly parallel to the chain axis but will have a distribution of inclinations, depending on the local sequence. There is also likely to be a distribution of carboxyl–aromatic torsion angles, which will contribute further to a distribution in monomer lengths. All of these effects need to be considered in refining the model to match the observed d spacings. The same distribution in monomer orientation will also tend to smooth the monomer transforms and thus will have some effect on the calculated intensities. In predicting intensities, our model is based on a single averaged chain and assumes there is no preferred axial chain stagger. However, the presence of sharp off-equatorial reflections indicates that there is some ordered lateral packing, and this could mean that there is a preferred axial stagger for some of the chains or monomer sequences. This will be considered as our calculations are expanded to consider the entire X-ray pattern, rather than simply the meridian, in order to develop three-dimensional models for the structures.

Acknowledgment. We thank Dr. J. B. Stamatoff of Celanese Research Co. for very useful discussions, and for providing the diffractometer data in Figure 8. This work is supported by Grants DMR81-07130, DMR81-19425, and ISI81-16103 from the National Science Foundation and from the Celanese Research Co.

Registry No. (HBA)·(DHN)·(TPA) (polymer), 78390-26-8; (HBA)·(HNA) (copolymer), 81843-52-9.

References and Notes

(1) J.-I. Jin, S. Antoun, C. Ober, and R. W. Lenz, *Br. Polym. J.*, **12**, 132 (1980).
(2) J. Blackwell and G. A. Gutierrez, *Polymer*, **23**, 671 (1982).
(3) G. A. Gutierrez, R. A. Chivers, J. Blackwell, J. B. Stamatoff, and H. Yoon, *Polymer*, **24**, 937 (1983).
(4) G. W. Calundann (Celanese), U.S. Patent 4 184 996, 1980.
(5) G. W. Calundann (Celanese), U.S. Patent 4 161 470, 1979.
(6) B. J. Adams and S. E. Morsi, *Acta Crystallogr., Sect. B*, **B32**, 1345 (1976).
(7) V. Pattabhi, S. Raghunathan, and K. K. Chacko, *Acta Crystallogr. Sect. B*, **B34**, 3118 (1978).
(8) J. P. Hummell and P. J. Flory, *Macromolecules*, **13**, 479 (1980).
(9) K. Tashiro, M. Kobayashi, and H. Tadokoro, *Macromolecules*, **10**, 413 (1977).
(10) B. K. Vainshtein, "Diffraction of X-rays by Chain Molecules", Elsevier, Amsterdam, 1966, p 312.
(11) J. Blackwell, G. Lieser, and G. A. Gutierrez, *Macromolecules*, **16**, 1418 (1983).
(12) G. A. Gutierrez and J. Blackwell, *Macromolecules*, in press.